P H Y S I C A L   R E V I E W   L E T T E R S

Phase Transitions in Definite Total Spin States of Two-Component Fermi Gases

Vladimir A. Yurovsky

School of Chemistry, Tel Aviv University, 6997801 Tel Aviv, Israel

Second-order phase transitions have no latent heat and are characterized by a change in symmetry. In addition to the conventional symmetric and antisymmetric states under permutations of bosons and fermions, mathematical group-representation theory allows for non-Abelian permutation symmetry. Such symmetry can be hidden in states with defined total spins of spinor gases, which can be formed in optical cavities. The present work shows that the symmetry reveals itself in spin-independent or coordinate-independent properties of these gases, namely as non-Abelian entropy in thermodynamic properties. In weakly interacting Fermi gases, two phases appear associated with fermionic and non-Abelian symmetry under permutations of particle states, respectively. The second-order transitions between the phases are characterized by discontinuities in specific heat. Unlike other phase transitions, the present ones are not caused by interactions and can appear even in ideal gases. Similar effects in Bose gases and strong interactions are discussed.

A distinctive feature of phase transitions is analytic discontinuities or singularities in the thermodynamic functions [1]. The transitions, analyzed here, are related to the permutation symmetry. According to the Pauli exclusion principle, the many-body wave function can be either symmetric of antisymmetric over particle permutations [2]. The particles can be either elementary—like electrons or photons—or composite—as atoms and molecules.

The symmetric and antisymmetric wave functions belong to one-dimensional irreducible representations (irreps) of the symmetric (or permutation) group [3]. However, group theory allows for the multidimensional, non-Abelian irreps of this group. They can be illustrated by many-body spin wave functions of electrons. A two-electron system with the total spin projection 0 has two states. In the first one, the first and the second electrons are in the spin up and spin down states, respectively, and vice versa in the second state. These two states can be symmetrized or antisymmetrized, giving the triplet and singlet states, respectively.

In the case of three electrons with the total spin projection $1/2$, each of them can be in the spin down state. This provides three nonsymmetric states. Symmetrization over permutations provides a one-dimensional irrep. However, the antisymmetric state does not exist, since two electrons are in the same spin up state. Then two three-body wave functions, which are orthogonal to the symmetric wave function, form a two-dimensional irrep.

Non-Abelian permutation symmetry has been considered in early years of quantum mechanics by Wigner [4], Heitler [5], and Dirac [6], before the Pauli exclusion principle was discovered. Particles with such symmetry, called "intermedions" were considered later and there are strong arguments that the total wave function cannot belong

to a non-Abelian irrep [7]. Nevertheless, if the spin and spatial degrees of freedom are separable, the total wave function, satisfying the Pauli principle, can be represented as a sum of products of spin and spatial wave functions with non-Abelian permutation symmetry. (Such wave functions are used in spin-free quantum chemistry [8,9], one-dimensional systems [10,11], and molecular relaxation [12].) Then spin-independent or coordinate-independent properties of such systems will be the same as those of hypothetical intermedions. The present work analyzes unusual thermodynamic properties arising from non-Abelian permutation symmetry.

A wave function can be symmetric or antisymmetric for any number of particles N. In contrast, the non-Abelian irrep matrices are specific for each N. Then the non-Abelian case can be described in canonical and microcanonical ensembles, but not in a grand canonical one. In a microcanonical ensemble [1], the macrostate of the gas is determined by N, the total energy E, the external potential or the volume where the particles are contained, and, in the present case, by the many-body spin S. According to the postulate of equal *a priori* probabilities [1], the system is equally likely to be in any microstate consistent with the given macrostate. The microstates are eigenstates of the many-body Hamiltonian. [An alternative derivation (see Supplemental Material [13]) is based on the Berry conjecture [19] rather than on the postulate of equal *a priori* probabilities].

Randomization of phases, due to either Hamiltonian chaos (as expressed by the Berry's conjecture [19,20]) or interactions with the environment, allows us to perform any unitary transformation of the microstates [1], namely, to eigenstates of noninteracting particles. For a gas of spin-$1/2$ fermions they are eigenstates of the Hamiltonian

$$\hat{H} = \hat{H}_{\text{spin}} + \hat{H}_{\text{spat}}, \qquad (1)$$

where $\hat{H}_{\text{spin}}$ is independent of the particle coordinates and $\hat{H}_{\text{spat}}$ is spin independent. Since the Hamiltonian (1) contains no terms that depend on both spins and coordinates, its eigenstates have the defined total spin S and can be represented as [13]

$$\tilde{\Psi}_{\hat{r}\{\varepsilon\}}^{(S)} = f_S^{-1/2}(N) \sum_t \tilde{\Phi}_{t\hat{r}\{\varepsilon\}}^{(S)} \Xi_t^{(S)}. \qquad (2)$$

Here the spatial $\tilde{\Phi}_{t\hat{r}\{\varepsilon\}}^{(S)}$ and spin $\Xi_t^{(S)}$ wave functions belong to conjugate irreps of the symmetric group. The irreps are associated with the Young diagram $[2^{N/2-S}, 1^{2S}]$, which is pictured as $N/2 - S$ rows with two boxes and $2S$ rows with one box [see, e.g, Figs. 2(a) and 2(b)]. The Young diagram is unambiguously determined by the total spin S and the irreps have the dimension $f_S(N)$ [13].

The functions within irreps are labeled by the standard Young tableaux t—the Young diagram $[2^{N/2-S}, 1^{2S}]$ filled by the numbers $1\ldots N$ which increase in each column and row from top to bottom and left to right, respectively [13]. The microstates are specified by the set of single-body energies $\{\varepsilon\} \equiv \{\varepsilon_1 \ldots \varepsilon_N\}$ and the Weyl tableau $\hat{r}$ [21]. The latter is a two-column Young diagram $[2^{N/2-S}, 1^{2S}]$ filled by ε_j such that they increase down each column but may be equal or increase left to right in each row [see Figs. 2(a) and 2(b)]. Then in the case of spin-1/2 fermions the set $\{\varepsilon\}$ can contain no more than double degeneracies. As proved in [13], the tableau $\hat{r}$ can take $f_S(q_1)$ values, where q_1 is the number of nondegenerate energies in the set $\{\varepsilon\}$. Then $f_S(q_1)$ can be considered as a statistical weight of the many-body state. Since the energies have to increase down the columns, the degenerate energies have to be placed in different columns, and the number of pairs of equal ε_j, $q_2 = (N - q_1)/2$, cannot exceed the shorter column length $N/2 - S$.

The eigenstates (2) with a defined total spin form a set of degenerate states with collective spin wave functions $\Xi_t^{(S)}$ and undefined spin projections of individual particles. The Hamiltonian (1) has also a set of degenerate eigenstates with the same energy but with defined individual spin projections and an undefined total spin. Given the total spin projection S_z (sum of individual spin projections), these sets can be connected by a unitary transformation.

Spin-independent interactions between particles split energies of the states with different total spins, making the set with defined individual spins inapplicable [5], but this effect is small for weakly interacting gases. A particular case of the states with defined total spins is the collective Dicke states [22] of two-level particles, coupled by an electromagnetic field in a cavity. A two-dimensional cavity leads to spin-dependent spatially homogeneous interactions of the form [23] $\hat{H}_{\text{spin}} = I\hat{S}_+\hat{S}_-$, where $\hat{S}_+$ and $\hat{S}_-$ are the total spin raising and lowering operators. Such interaction, realized in recent experiments [24], lead to the energy shift
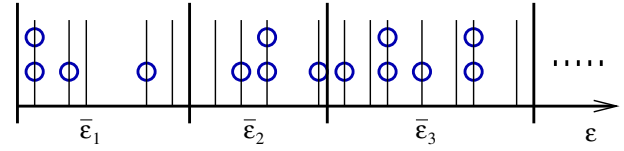

FIG. 1. Cells with average energies $\bar{\varepsilon}_i$ in a single-body energy spectrum. The circles denote the level occupation.

$E_{SS_z} = I[S_z(S_z - 1) - S(S + 1)]$, providing substantial splitting of the states with different total spins [13].

The protocol, proposed in [25], starts from the spin-polarized state with $S = S_z = N/2$. A time-dependent potential, which changes the spin states of particles, but, being coordinate independent, conserves the total spin, can transfer the population to the state with $S = N/2$, $S_z = N/2 - 1$. Later a potential, which does not change the spin states of particles, can, being dependent on coordinates and spins, transfer the population to the state with $S = N/2 - 1$, $S_z = N/2 - 1$. A sequence of such pulses with proper time-dependencies can populate the state with any total spin. The population will not be transferred back to higher S and S_z, since the energy spectrum E_{SS_z} is not equidistant and, therefore, $E_{SS_z} - E_{SS_z-1} \neq E_{SS_z+1} - E_{SS_z}$ and $E_{SS_z} - E_{S-1S_z} \neq E_{S+1S_z} - E_{SS_z}$.

Following the Gentile's version [26] of the general microcanonical approach, let us divide the single-body energy spectrum into cells (see Fig. 1) containing g_i energy levels with the average energy $\bar{\varepsilon}_i$. Let $q_0^{(i)}$, $q_1^{(i)}$, and $q_2^{(i)}$ levels be, respectively, nonoccupied, single occupied, and double occupied in the ith cell. Given these occupations, the levels in the cell can be distributed in $g_i!/(q_0^{(i)}!q_1^{(i)}!q_2^{(i)}!)$ distinct ways [26]. Then the number of distinct microstates associated with the sets $q_l^{(i)}$ is $f_S(q_1)\prod_i g_i!/(q_0^{(i)}!q_1^{(i)}!q_2^{(i)}!)$. The system configuration corresponds to the most-probable values of $q_l^{(i)}$ [13]. They maximize the number of microstates, or its logarithm—entropy

$$H = \sum_i \left(g_i \ln g_i - \sum_{l=0}^{2} q_l^{(i)} \ln q_l^{(i)} \right) + \ln f_S(q_1). \quad (3)$$

Here the Stirling approximation is used. The number of nondegenerate energies ε_j in the set $\{\varepsilon\}$ is equal to the total number of single-occupied levels $q_1 = \sum_i q_1^{(i)}$. The sum in Eq. (3) gives the entropy of the Gentile gas [26]. The present results follow from the last term, which will be referred to as non-Abelian entropy, since it vanishes when $f_S = 1$.

A permutation of single-body energies in the set $\{\varepsilon\}$ transforms [6,8] the wave function (2) to a linear combination of $\tilde{\Psi}_{\hat{r}\{\varepsilon\}}^{(S)}$ with different $\hat{r}$. The Weyl tableaux $\hat{r}$ are unambiguously related to the Young tableaux of the shape
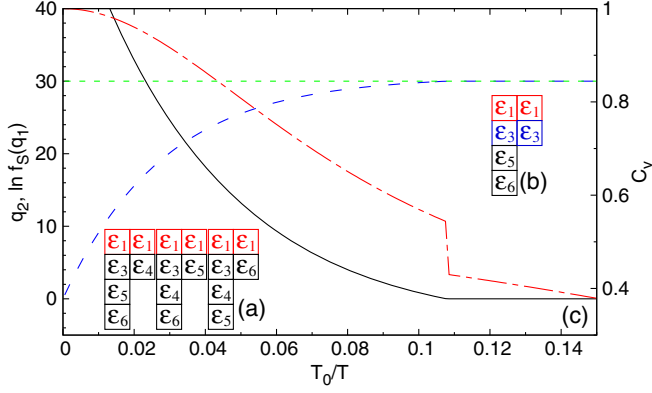
FIG. 2. (a) Three allowed Weyl tableaux for $\varepsilon_1 = \varepsilon_2 < \varepsilon_3 < \varepsilon_4 < \varepsilon_5 < \varepsilon_6$ corresponding to the unsaturated phase. The black cells form Young tableaux corresponding to a non-Abelian irrep. (b) A Weyl tableau for $\varepsilon_1 = \varepsilon_2 < \varepsilon_3 = \varepsilon_4 < \varepsilon_5 < \varepsilon_6$ corresponding to the saturated phase. The black cells form a one-column Young tableau corresponding to an antisymmetric irrep. (c) The total number of double-occupied levels q_2 (blue long dash), the maximal allowed value of q_2 (green horizontal short dash), non-Abelian entropy $\ln f_S(q_1)$ (black solid line), and specific heat (per atom) C_v (red dotted-dashed line) at the temperature T for $N = 10^2$ two-dimensional particles in a flat potential with the total spin $S = 20$. The temperature scale T_0 is given by Eq. (4).

FIG. 3. Specific heat (per atom) at the temperature T for the state with the defined many-body spin S (black solid lines) and the state with defined individual spins and the total spin projection $S_z = S$ (red dashed lines) of $N = 10^2$ two-dimensional particles in a flat potential. The blue line shows the boundary between the saturated (S) and unsaturated (U) phases. The temperature scale T_0 is given by Eq. (4).

$[2^{N/2-S-q_2}, 1^{2S}]$ obtained by the crossing out of the q_2 degenerate pairs of ε_j from the Weyl tableaux with $N/2 - S$ two-box rows [13]. Then the wave functions $\tilde{\Psi}^{(S)}_{\hat{r}\{\varepsilon\}}$ form an irrep, associated with the Young diagram $[2^{N/2-S-q_2}, 1^{2S}]$, of the group S_{q_1} of permutations of nondegenerate ε_j. In the saturated phase, $q_2 = N/2 - S$, the diagram has one column [see Fig. 2(b)], the irrep is Abelian, and the many-body state has the statistical weight $f_S(2S) = 1$. The unsaturated phase ($q_2 < N/2 - S$) corresponds to the non-Abelian irreps [see Fig. 2(a)]. At high temperatures, when the number of double-occupied levels q_2 is small, the system is in the unsaturated phase. On the temperature decrease, q_2 increases, while the statistical weight $f_S(q_1)$ decreases [see Fig. 2(c)]. At the critical temperature q_2 reaches the maximal allowed value $N/2 - S$, the system transforms to the saturated phase, and $f_S(q_1)$ has a corner. This leads to discontinuity of the specific heat (per atom) $C_v = (\partial E/\partial T)_V/N$ (see Figs. 2(c) and 3 and [13]). The transition is characterized by the non-Abelian entropy $\ln f_S(q_1)$, which ranges between zero in the saturated phase and nonzero in the unsaturated one. However, $\ln f_S(q_1)$ is not a local order parameter. Rather, it is a topological characteristic of the collective state.

The conventional state with defined individual spins is a mixture of two gases containing $N/2 + S_z$ and $N/2 - S_z$ particles, respectively, with Fermi-Dirac distributions. It is a superposition of all states with defined total spins $S \le S_z$. As the statistical weight $f_S(N)$ attains its maximum at $S = \sqrt{N+2}/2$, the state with $S = S_z$ dominates in this
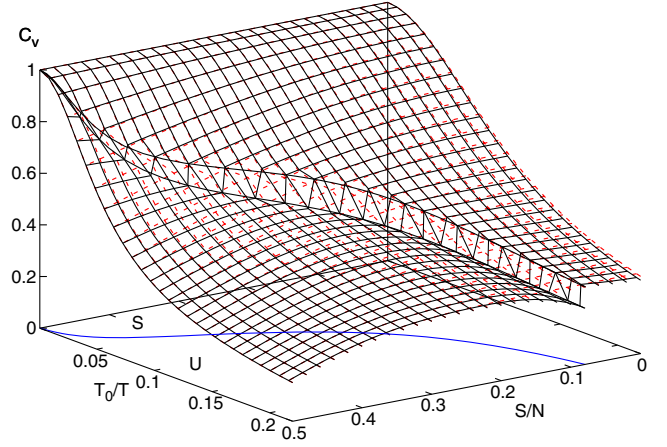
superposition, unless $S_z \lesssim \sqrt{N}$. However, thermodynamic properties of each S-component in this superposition are determined by the maximum of the mixture entropy, which is different from Eq. (3). Then none of the S components is in its thermal equilibrium. As a result, thermodynamic properties of the mixture and of the non-Abelian state with $S = S_z$ are different, and the mixture does not demonstrate the phase transition (see Fig. 3 and [13]).

The present phase transition has no latent heat since the energy, as well as entropy and pressure, is continuous [13]. It is therefore a second-order phase transition, like the well-known superconducting one in the absence of magnetic fields. However, the latter is a result of interactions between particles, while the present phase transition can take place in an ideal gas. In this sense, it is similar to the Bose-Einstein condensation phase transition, where the specific heat is discontinuous in the special case of a gas in a 3D harmonic trap [27,28]. In contrast, the present phase transition takes place in trapped and free gases of any dimension (see Fig. 3 and [13]). Figures 4(a) and 4(b) show the specific heat at the phase boundary, which is discontinuous and different from the one for defined individual spins. Being plotted as a function of the scaled temperature $T/T_k(N)$, it demonstrates small variation when the trapping and dimensionality are changed [see Figs. 4(b) and 4(c)]. Here the temperature scale is

$$T_k(N) = \nu_k^{-1/(k+1)} N^{-k/(k+1)} \qquad (4)$$

and k is the parameter in the energy density of single-body levels $\nu(\varepsilon) = \nu_k \varepsilon^k$ (for the 2D and 3D gases in flat potentials $k = 0$ and $1/2$, respectively, while $k = 1$ and
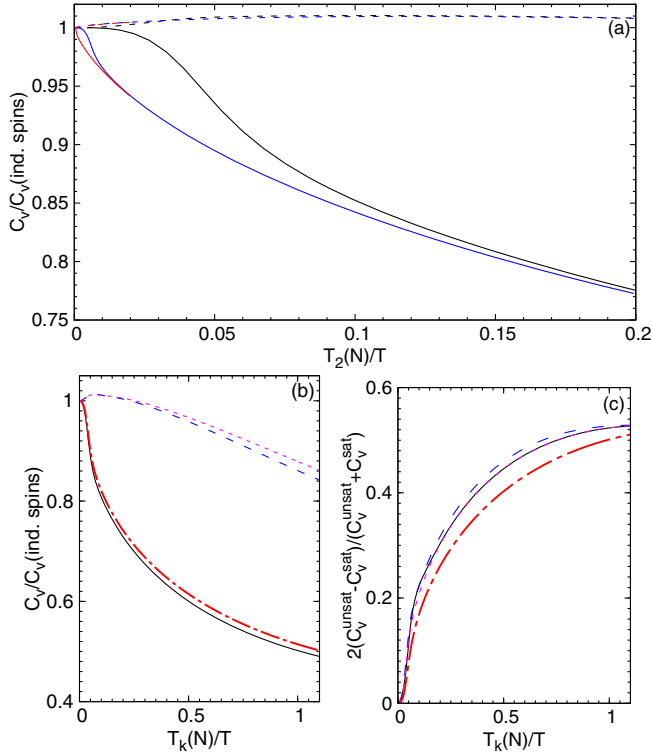
FIG. 4. (a) The ratio of the specific heat on the phase boundary to the one for the gas with defined individual spins in a three-dimensional (3D) harmonic trap for the saturated (solid lines) and unsaturated (dashed lines) phases with $N = 10^2$ (black), $N = 10^3$ (blue), and $N = 10^4$ (red) particles. The temperature scale $T_k(N)$ is defined by Eq. (4). (b) The same ratios for the 3D gas in a flat potential; the black solid and blue long-dashed lines correspond to the saturated and unsaturated phases, respectively. The ratios for a two-dimensional (2D) harmonic trapping are plotted by the red dotted-dashed and magenta short-dashed lines, respectively. All plots are for $N = 10^2$. (c) The relative change in the specific heat at the phase boundary for $N = 10^2$ particles in flat potentials (black solid and blue long-dashed lines for the 2D and 3D cases, respectively) and in harmonic traps (red dotted-dashed and magenta short-dashed lines, respectively).

2 for the 2D and 3D harmonic trapping, respectively [13]). The plots for different numbers of particles converge on the decrease of the scaled temperature [see Fig. 4(a)]. The temperature scale is related to the Fermi energy defined by the equation $\int_0^{\varepsilon_F} \nu_k \varepsilon^k d\varepsilon = N$ as $\varepsilon_F = [(k+1)N/\nu_k]^{1/(k+1)}$. Then the average energy density ε_F/N is, up to a factor, the temperature scale (4). Figure 4(c) shows that the relative change of the specific heat at the phase boundary approaches 0.5 at $T < T_k(N)$ for any trapping and dimensionality. Except of the case of a free 2D gas, the temperature scale decreases with increase of N. Then the more particles are in the gas, the lower the temperature required in order to observe the phase transition. Even in a free 2D gas, the required temperature decreases in the thermodynamic limit, when $N \to \infty$ with the fixed density N/V_{2D},

since $\nu_0 \propto V_{2D}$ tends to infinity [13] and, therefore, $T_0(N) \to 0$. In this sense, the phase transition is a mesoscopic effect (see the discussion in the end of [13]).

In Gentile's intermediate statistics [26], each single-body state can be occupied by a limited number of particles. If this limit is two, Gentile's statistics leads to Eq. (3) with $f_S \equiv 1$ and $S = 0$, when the two columns of the Young diagram have equal length. For $S = 0$, as demonstrated above, the transition temperature tends to zero and the gas is in the unsaturated phase at finite temperatures. Then the phase transition, considered here, cannot appear in Gentile's statistics. Another reason is that the condition $f_S \equiv 1$ eliminates the non-Abelian entropy and any connection between occupations of single-body states. The non-Abelian entropy depends on the total number of single-occupied states and is not an extensive nor an intensive property, being related to the collective state of the gas.

Zero-range two-body interactions in cold spin-$1/2$ Fermi gases are spin independent, since collisions of atoms in the same spin state are forbidden by the Pauli principle. The interactions become spin dependent and spin and spatial degrees of freedom become inseparable due to inapplicability of the zero-range approximation when the de Broglie wavelength becomes comparable to the effective interaction radius $r_{\rm eff}$ [13]. Then the atom energy is restricted by ~ 40 mK for ^{6}Li atoms (the limiting energy is inversely proportional to the atom mass). Under the same condition, the gas can be considered as weakly interacting and the formation of dimers or Cooper pairs for repulsive or attractive interactions, respectively, can be neglected [13], since the elastic scattering length is $|a_S| \approx r_{\rm eff}$ for nonresonant interactions.

However, the spin and spatial degrees of freedom can be separated for interactions of arbitrary strength while they are spin independent, and the gas can be kept in a state with the defined many-body spin. For example, in the case of cold atoms, Feshbach resonances [27–29] can provide large a_S for zero-range interactions, leading to non-negligible formation of dimers or Cooper pairs. Since they are symmetric over permutations of forming-particle's coordinates, the number of dimers and Cooper pairs will be restricted by $N/2 - S$. This can lead to phase transitions in strongly interacting gases too, although particles do not occupy single-body states.

In high-spin Fermi gases, similar phase transitions can appear when the interactions are spin independent, as in $SU(n)$ gases [30–35]. If the spatial state of such gas is associated with a Young diagram with nonequal column lengths, a phase transition can be expected when the number of levels occupied by l particles approaches the lth column length.

Bose gases with spin-independent interactions allow for the separation of spin and spatial degrees of freedom, and their states can be associated with Young diagrams too. Such states of spin-$1/2$ bosons were analyzed [36,37] using

$SU(2)$ symmetry [irreps of $SU(2)$ and symmetric groups are closely related, having common basic functions]. In the ground state, all particles occupy two lowest levels [36,37]. Non-Abelian entropy can lead to a phase transition when the occupation of the lowest level approaches the first row length $N/2 + S$. For high-spin bosons, phase transitions can be expected when the occupation of the nth excited level approaches the length of $n + 1$th row. A certain analogy can be drawn to the phase transitions in coupled tubes controlled by the tube filling factors [38].

States with non-Abelian symmetry can find applications in quantum metrology, computing and information processing, like non-Abelian anyons related to representations of the braid group [39,40]. Thermodynamical properties of an ideal gas of non-Abelian anyons studied in [41] do not demonstrate phase transitions.

In conclusion, eigenstates of two-component Fermi gases have defined many-body spins and can be associated with multidimensional, non-Abelian irreps of the symmetric group. An additional energy degeneracy of the eigenstates modifies the system entropy, leading to second-order phase transitions in the case of weak interactions.

[1] R. K. Pathria and P. D. Beale, *Statistical Mechanics* (Elsevier Science, New York, 2011).

[2] L. D. Landau and E. M. Lifshitz, *Quantum Mechanics: Non-Relativistic Theory* (Pergamon Press, New York, 1977).

[3] M. Hamermesh, *Group Theory and Its Application to Physical Problems* (Dover, Mineola, NY, 1989).

[4] E. Wigner, Über nicht kombinierende terme in der neueren quantentheorie. II. Teil, Z. Phys. **40**, 883 (1927).

[5] W. Heitler, Störungsenergie und austausch beim mehrkörperproblem, Z. Phys. **46**, 47 (1927).

[6] P. A. M. Dirac, Quantum mechanics of many-electron systems, Proc. R. Soc. A **123**, 714 (1929).

[7] I. G. Kaplan, The Pauli exclusion principle. Can it be proved?, Found. Phys. **43**, 1233 (2013).

[8] I. G. Kaplan, *Symmetry of Many-Electron Systems* (Academic Press, New York, 1975).

[9] R. Pauncz, *The Symmetric Group in Quantum Chemistry* (CRC Press, Boca Raton, 1995).

[10] C. N. Yang, Some Exact Results for the Many-Body Problem in One Dimension with Repulsive Delta-Function Interaction, Phys. Rev. Lett. **19**, 1312 (1967).

[11] B. Sutherland, Further Results for the Many-Body Problem in One Dimension, Phys. Rev. Lett. **20**, 98 (1968).

[12] S. D. Brechet, F. A. Reuse, K. Maschke, and J.-P. Ansermet, Quantum molecular master equations, Phys. Rev. A **94**, 042505 (2016).

[13] See Supplemental Material at http://link.aps.org/supplemental/10.1103/PhysRevLett.118.200403, which includes Refs. [14–18], for derivation details and supporting information.

[14] J. Nocedal and S. Wright, *Numerical Optimization* (Springer, New York, 2006).

[15] T. Kinoshita, T. Wenger, and D. S. Weiss, A quantum Newton's cradle, Nature (London) **440**, 900 (2006).

[16] V. A. Yurovsky, Long-lived states with well-defined spins in spin-1/2 homogeneous Bose gases, Phys. Rev. A **93**, 023613 (2016).

[17] F. W. Olver, D. W. Lozier, R. F. Boisvert, and C. W. Clark, *NIST Handbook of Mathematical Functions* (Cambridge University Press, Cambridge, England, 2010).

[18] Z. Gong, L. Zejda, W. Däppen, and J. M. Aparicio, Generalized Fermi-Dirac functions and derivatives: properties and evaluation, Comput. Phys. Commun. **136**, 294 (2001).

[19] M. V. Berry, Regular and irregular semiclassical wavefunctions, J. Phys. A **10**, 2083 (1977).

[20] M. Srednicki, Chaos and quantum thermalization, Phys. Rev. E **50**, 888 (1994).

[21] N. L. Harshman, One-dimensional traps, two-body interactions, few-body symmetries. II. N particles, Few-Body Syst. **57**, 45 (2016).

[22] R. H. Dicke, Coherence in spontaneous radiation processes, Phys. Rev. **93**, 99 (1954).

[23] E. Sela, V. Fleurov, and V. A. Yurovsky, Molecular spectra in collective Dicke states, Phys. Rev. A **94**, 033848 (2016).

[24] R. Landig, L. Hruby, N. Dogra, M. Landini, R. Mottl, T. Donner, and T. Esslinger, Quantum phases from competing short- and long-range interactions in an optical lattice, Nature (London) **532**, 476 (2016).

[25] V. A. Yurovsky, Permutation Symmetry in Spinor Quantum Gases: Selection Rules, Conservation Laws, and Correlations, Phys. Rev. Lett. **113**, 200406 (2014).

[26] G. Gentile, Osservazioni sopra le statistiche intermedie, Il Nuovo Cimento **17**, 493 (1940).

[27] L. Pitaevskii and S. Stringari, *Bose-Einstein Condensation and Superfluidity* (University Press, Oxford, England, 2016).

[28] C. J. Pethick and H. Smith, *Bose-Einstein Condensation in Dilute Gases* (Cambridge University Press, Cambridge, England, 2008).

[29] C. Chin, R. Grimm, P. Julienne, and E. Tiesinga, Feshbach resonances in ultracold gases, Rev. Mod. Phys. **82**, 1225 (2010).

[30] C. Honerkamp and W. Hofstetter, Ultracold Fermions and the $SU(N)$ Hubbard Model, Phys. Rev. Lett. **92**, 170403 (2004).

[31] A. V. Gorshkov, M. Hermele, V. Gurarie, C. Xu, P. S. Julienne, J. Ye, P. Zoller, E. Demler, M. D. Lukin, and A. M. Rey, Two-orbital $SU(N)$ magnetism with ultracold alkaline-earth atoms, Nat. Phys. **6**, 289 (2010).

[32] M. A. Cazalilla, A. F. Ho, and M. Ueda, Ultracold gases of ytterbium: Ferromagnetism and Mott states in an $SU(6)$ Fermi system, New J. Phys. **11**, 103033 (2009).

[33] X. Zhang, M. Bishof, S. L. Bromley, C. V. Kraus, M. S. Safronova, P. Zoller, A. M. Rey, and J. Ye, Spectroscopic observation of $SU(N)$-symmetric interactions in Sr orbital magnetism, Science **345**, 1467 (2014).

[34] G. Pagano, M. Mancini, G. Cappellini, P. Lombardi, F. Schaefer, Hui Hu, X.-J. Liu, J. Catani, C. Sias, M. Inguscio, and L. Fallani, A one-dimensional liquid of fermions with tunable spin, Nat. Phys. **10,** 198 (2014).

[35] F. Scazza, C. Hofrichter, M. Höfer, P. C. De Groot, I. Bloch, and S. Fölling, Observation of two-orbital spin-exchange interactions with ultracold $SU(N)$- symmetric fermions, Nat. Phys. **10,** 779 (2014).

[36] A. B. Kuklov and B. V. Svistunov, Ground States of $SU(2)$-Symmetric Confined Bose Gas: Quantum Superposition of the Phase-Separated Classical Condensates, Phys. Rev. Lett. **89,** 170403 (2002).

[37] S. Ashhab and A. J. Leggett, Bose-Einstein condensation of spin-1/2 atoms with conserved total spin, Phys. Rev. A **68,** 063612 (2003).

[38] A. Safavi-Naini, B. Capogrosso-Sansone, and A. Kuklov, Quantum phases of hard-core dipolar bosons in coupled one-dimensional optical lattices, Phys. Rev. A **90,** 043604 (2014).

[39] A. Stern and N. H. Lindner, Topological quantum computation–from basic concepts to first experiments, Science **339,** 1179 (2013).

[40] S. M. Albrecht, A. P. Higginbotham, M. Madsen, F. Kuemmeth, T. S. Jespersen, J. Nygard, P. Krogstrup, and C. M. Marcus, Exponential protection of zero modes in Majorana islands, Nature (London) **531,** 206 (2016).

[41] F. Mancarella, A. Trombettoni, and G. Mussardo, Statistical mechanics of an ideal gas of non-Abelian anyons, Nucl. Phys. **B867,** 950 (2013).